

Brazilian tests and tensile strength of the sea and fresh water ice

R. Izimov¹, A. Sakharov¹, E. Karulin², A. Marchenko^{3,4}, M. Karulina², P. Chistyakov¹

¹ Moscow State University, Moscow, RUSSIA

² Krylov State Research Centre, St.-Petersburg, RUSSIA

³ The University Centre in Svalbard, Longyearbyen, Norway

⁴ Norwegian University of Science and Technology, Trondheim, Norway

ABSTRACT

This article discusses the use of the Brazilian test to study the strength characteristics of ice. The experimental stress-strain curves obtained during the Brazilian tests of cylindrical ice samples gave an unambiguous picture of sample destruction (splitting of the sample into two parts), the scattering of experimental data was less than 5%. At the same time, during tests by the direct method, it was not possible to obtain a definite value of the ultimate stress at which fracture occurs. Wing-cracks are characteristic defects in materials such as rocks and ice. The paper describes the numerical modeling of rectangular samples weakened by one isolated wing-crack under the action of compressive forces applied at the ends, and cylindrical samples in the Brazilian test for the analysis of mechanisms characterizing the failure of samples.

KEY WORDS: Ice; Failure; Brazilian Test; Wing crack; Stress intensity factor.

INTRODUCTION

The Brazilian test is a simple indirect testing method to obtain the tensile strength of brittle material such as concrete, rock, and rock-like materials. In this test, a thin circular disc is diametrically compressed to failure.

The compression induces tensile stresses normal to the vertical diameter, which are essentially constant over a region around the center. The indirect tensile strength is typically calculated based on the assumption that failure occurs at the point of maximum tensile stress, i.e., at the center of the disc. The suggested formula for calculating the splitting tensile strength based on the Brazilian test is

$$\sigma_p = \frac{2P}{\pi D L} \quad (1)$$

where P is the load at failure, D is the diameter of the test sample, and L is the thickness of the test sample measured.

In this paper, we discuss the use of the Brazilian test to study the strength characteristics of ice. The experimental stress-strain curves obtained during the Brazilian tests of cylindrical ice samples gave an unambiguous picture of sample destruction (splitting of the sample into two parts).

The strength of ice at brittle fracture is due to the initiation and propagation of cracks. The second part of the paper is devoted to the analysis of the influence of wing cracks on the fracture

process. Wing-crack propagation is described by the stress-driven crack model. Due to shear, tensile forces are generated along the sliding area and the crack behaves like a normal pull-off crack.

The paper describes the numerical modeling of rectangular samples weakened by one isolated wing-crack under the action of compressive forces applied at the ends, and cylindrical samples in the Brazilian test for the analysis of mechanisms characterizing the failure of samples.

EXPERIMENTS

The experiments described below will help us demonstrate how the Brazilian test may be applied to studying the strength characteristics of the fresh and sea water ice.

Tests of a series of cylindrical ice samples of the same type by the Brazilian method gave an unambiguous picture of destruction - splitting of the sample into two equal parts along the compressed diameter. Figures 1 and 2 show samples of fresh and sea ice at different stages of the experiment, respectively.

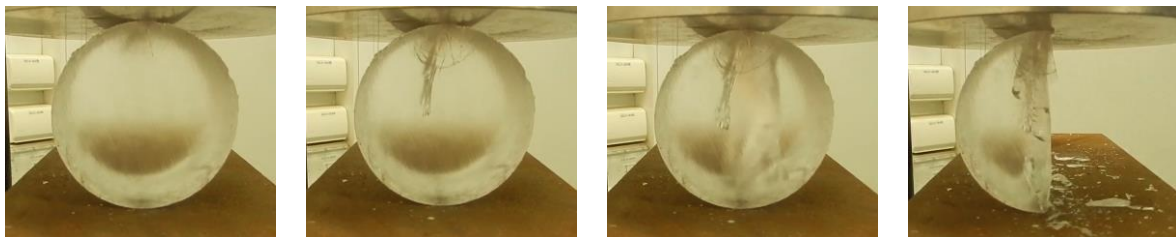


Figure 1. The process of failure of the freshwater ice in the Brazilian test

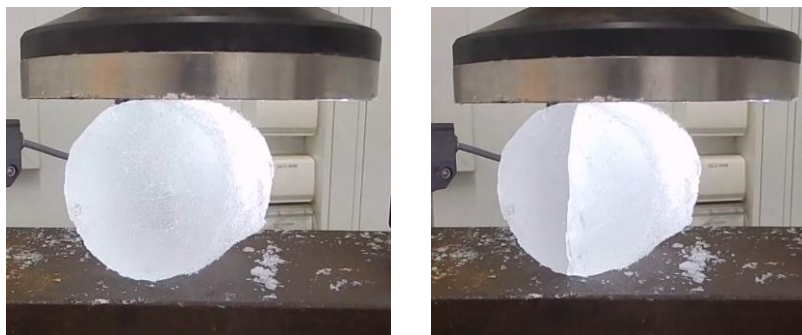


Figure 2. The process of failure of the sea ice in the Brazilian test

Below are the results of determining the tensile strength using the Brazilian test.

Table 1. The characteristics of the experiments of fresh water ice

Test #	Core №.	d, mm	l,mm	P*, N	σ_t , Mpa
1	1	72	70	3173	0,40
2	1	72	70	4231	0,53
4	2	72	70	3150	0,40
7	2	72	70	4109	0,52
8	2	72	70	3209	0,41
9	3	72	70	2470	0,31
10	3	72	70	2551	0,32

Table 2. The characteristics of the experiments of sea water ice

Test #	Core №.	d, mm	l,mm	P*, N	σ_t , MPa
1	1	72	70	2477	0,31
2	1	72	70	1922	0,24
3	1	72	70	2661	0,34
1_1	2	72	70	2807	0,35
1_2	2	72	70	2448	0,31
1_3	2	72	70	1644	0,21
2_1	2	72	70	2803	0,35
2_2	2	72	70	3820	0,48
2_3	2	72	70	3649	0,46
2_4	2	72	70	2447	0,31
3_1	3	72	70	3021	0,38
3_2	3	72	70	3309	0,42
4_1	3	72	70	2968	0,37
5_1	3	72	70	1909	0,24
5_2	3	72	70	3145	0,40
5_3	3	72	70	2607	0,33
5_4	3	72	70	1971	0,25

Experimental results analysis

Stress evaluation was performed according to the analytical solution of the circular disk stress problem (Timoshenko S.P., Goodyear J. Theory of elasticity. M.: Nauka, 1975. 757 p.).

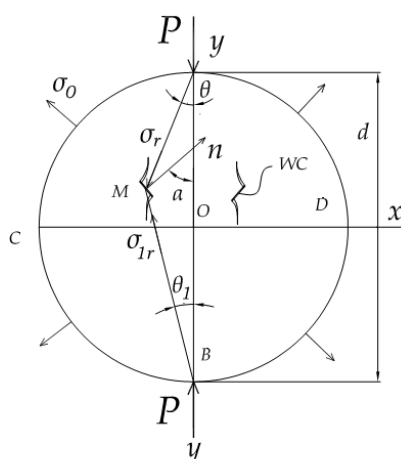


Figure 3. Stress field in Brazilian test

The solution of the problem is the superposition of three stress fields:

1. radial top stress field

$$\sigma_r = -\frac{2 P \cos \theta}{\pi r} \quad (2)$$

2. radial bottom stress field

$$\sigma_r = -\frac{2 P \cos \theta}{\pi r} \quad (3)$$

3. comprehensive tension

$$\sigma^0 = -\frac{P}{\pi r} \quad (4)$$

Thus, there will be areas in the disk where for each placement of a platform there will be enough friction force to press down the sliding area. These areas can be found analytically. These safe areas will be at the periphery of the disk; no cracks can form there.

In the danger zone, it is necessary to exclude "pole caps" (load points) because another elastic solution - the Hertz contact problem applies there, which is not covered by the solution of this stress field.

In the remaining area it is necessary to take a crack no larger than the size d of the grain, and take the size of the area according to Sanderson $2 l_0 \sim 0,65 d$, and in the remaining area isolate the zones where the coefficient of intensity for an isolated crack is less than K_{1C} .

Then the entire disk is divided into areas where different conditions are met. This can be done very roughly. Since it is intuitively clear that we are interested in the area along the central diameter, we can also solve the field equations (2), (3), (4) analytically in this area for an isolated crack. This will give us an explanation of why the wings of the crack develop toward the center of the disk, and not toward the poles. Then it is necessary to account for the chains of cracks, because each winged one is stable and does not produce splitting.

The paper Stepanova L.V., and Dolgikh V. S. (2017) presents the results of experiments on circular samples. Figure 4 shows the pattern of interfering bands in the disc loaded 210 kg. Since isochromes determine the difference in the values of the principal stresses, they can be used to analyze whether or not the sliding area would be in the danger zone, if it were there. In Figure 4 we can clearly see the area at the pole where the stress field corresponds to the Hertz contact problem.

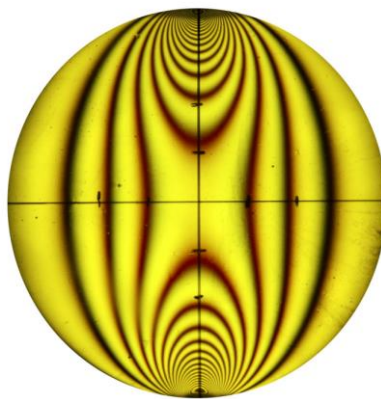


Figure 4. Loading the sample with 210 kg

NUMERICAL ANALYSIS

The problem considered here is two-dimensional. Figure 5 shows the configuration to be modeled. From an initially present crack of length $2l_0$, two tensile wing cracks have grown to a length l , driven by a slide along the initial crack.

The remotely applied stress field is $\sigma = \sigma_{11}e_1 + \sigma_{22}e_2$, where e_1, e_2 are unit vectors.

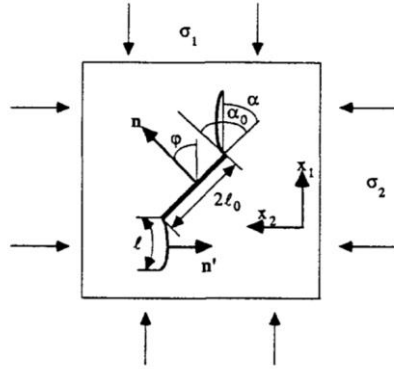


Figure 5. The winged crack configuration

Computational parameters

Three parameters are considered in this study for investigating the crack growth behaviour:

1. $L = l / l_0$ is wing crack length to initially present fracture length ratio
2. ϕ - angle of inclination of the main crack to the axis x
3. μ - friction coefficient of the sliding area

Simulation results analysis and discussions

In the numerical simulation of a rectangular sample weakened by an isolated crack, during the transition from short to long wing asymptotic, the picture of the distribution of normal stresses on the sliding area changes. When the parameter $L > 1$, the distribution of stresses corresponds to the problem of embedding a die in an elastic half-plane (Prandtl problem). The figure 6 shows the distribution of normal stresses for different values of the parameter L .

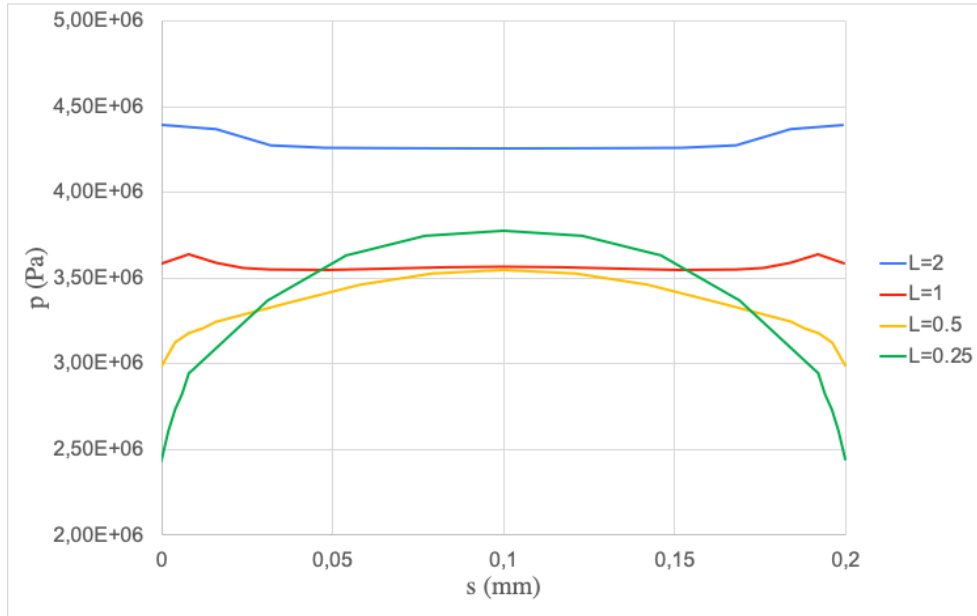


Figure 6. Transition from the problem of shear along the sliding area to the contact problem

Wing-crack propagation is described by the stress-driven crack model. Due to shear, tensile forces are generated along the slide and the crack behaves like a normal pull-off crack in conjunction with condition:

$$K_{1c} = K_1 \quad (5)$$

In numerical modeling, we obtained a non-zero value of the stress intensity factor K_2 , which corresponds to the behavior of a longitudinal shear crack. Moreover, the value of the coefficient K_2 is of the same order as the value of the coefficient K_1 . The graph below shows the ratio of the coefficients for various parameters of numerical simulation.

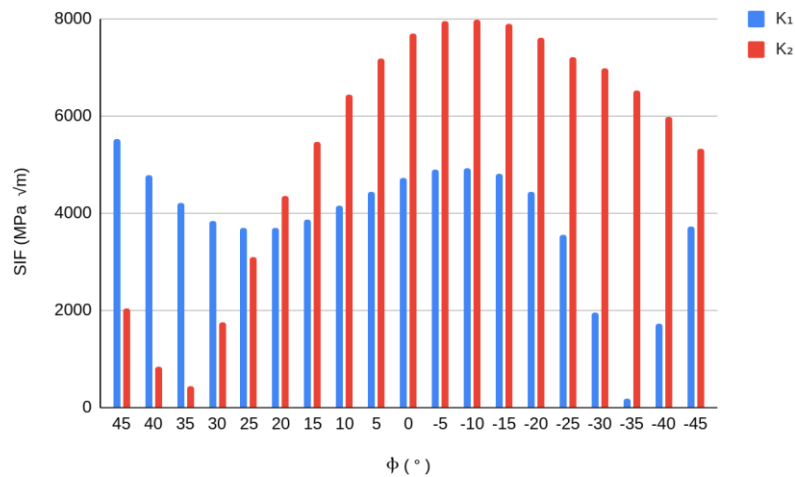


Figure 7. Parametric Analysis

Numerical analysis validation

The paper Lehner, F., Kachanov, M. (1996) presents an overview of analytical formulas for calculating the stress intensity factor for the configuration shown in Figure 3. To assess the influence of the parameters on crack growth behavior we consider the following models:

- A. stress-driven crack model

$$K_{\square} = \frac{(\tau + \mu \sigma_{nn}) 2 l_0 \cos(\varphi)}{\sqrt{\pi l}} \quad (6)$$

B. model of short wing asymptotics

$$K_{\square} = (2 / \sqrt{3}) (\tau + \mu \sigma_{nn}) \sqrt{\pi l_0} \quad (7)$$

C. model of the entire range of wing lengths

$$K_{\square} = \frac{(\tau + \mu \sigma_{nn}) 2 l_0 \cos(\varphi)}{\sqrt{\pi (l + 3 l_0 \pi^{-2} \cos^2(\varphi))}} \quad (8)$$

Table 4 shows a comparison of the value of the K_1 , obtained by numerical simulation, with the analytical formulas from [1].

Table 4. Convergence of the numerical solution to analytical estimates for the K_1

L	Model A	Model B	Model C
5	0,774	0,853	0,768
2	0,628	0,712	0,605
1	0,0491	0,398	0,071
0.5	0,142	0,241	0,062
0.25	0,346	0,162	0,058

For short wing asymptotics, the obtained results are excellent. The difference between numerical and analytical values is less than 10 percent.

For a long wing asymptotics crack, however, the value of the coefficient obtained by numerical modeling differs strongly from the analytical one. This may be due to the fact that at large values of the parameter L , the stress distribution on the sliding area is more consistent with the stress distribution for the contact problem, when the maximum of normal stresses is reached at the boundary of the elastic foundation.

CONCLUSIONS

From a series of Brazilian tests on samples of the sea and fresh water ice, we address the application of the Brazilian test to study the strength characteristics of ice. The main conclusions are as follows:

- A. The experimental stress-strain curves obtained during the Brazilian tests of cylindrical ice samples gave an unambiguous picture of sample destruction (splitting of the sample into two parts).
- B. A problem with the experiments is that cracks are initiating and propagating from the loading point at the top of the cylinder in Figure 1. This is a problem with the Brazilian test method that has been discussed in the literature and that researchers have tried to mitigate by utilizing shaped strip/pads at the contact loading regions or by flattening the contact areas on the ice cylinders to some extent to avoid crack-initiating stress concentrations at the contact zones.

- C. Proceeding with photoelastic stress analysis to determine the positions of the failure area sites by WC. The frequency of isochromes will help us determine the crack growth rate as long as it runs from the zone of concentration (at the pole) to the center, where everything is uniform.

The main results obtained in the numerical simulation of samples weakened by a wing-crack:

- A. Wing-crack propagation is described by the stress-driven crack model, it has been assumed that the crack propagates like a normal pull-off crack. This assumption was not prompted by numerical simulation of the problem. In numerical modeling, we obtained a non-zero value of the stress intensity factor K_2 , which corresponds to the behavior of a longitudinal shear crack.

REFERENCES

Chistyakov P., Karulin E., Marchenko A., Sakharov A., Lishman B., 2016. Tensile strength of the saline and freshwater ice in field tests. *23^d IAHR International Symposium on Ice, Ann Arbor, U.S.A.: Michigan.*

Dykens, J E., 1970. Ice engineering: tensile properties of sea ice grown in a confined system. *Port Hueneme, CA, Naval Civil Engineering Laboratory. U.S.A.: California.*

Kuehn, G. A., Lee, R. W., Nixon, W. A., and Schulson, E. M., 1990. The Structure and Tensile Behavior of First-Year Sea Ice and Laboratory-Grown Saline Ice. *ASME. J. Offshore Mech. Arct. Eng.*, 112(4): pp.357–363.

Lehner, F., Kachanov, M., 1996. On modelling of “winged” cracks forming under compression. *Int J Fract* 77, pp. 69–75.

M. Cai, P.K Kaiser, 2004. Numerical Simulation Of The Brazilian Test And The Tensile Strength Of Anisotropic Rocks And Rocks With Pre-Existing Cracks. *International Journal of Rock Mechanics and Mining Sciences*, pp.478-483.

Menge, J., & Jones, K., 1993. The tensile strength of first-year sea ice. *Journal of Glaciology*, 39(133), pp.609-618.

Sanderson T. J. O., 1998. *Ice Mechanics and Risks to Offshore Structures*. Graham and Trotman:London.

Stepanova L.V., and Dolgikh V. S., 2017. “Experimental determination of the coefficients of multiparametric decomposition of the stress field at the crack tip: the photoelasticity method” (in Russian "Экспериментальное определение коэффициентов многопараметрического разложения поля напряжений у вершины трещины: метод фотоупругости") *Vestnik of Samara University. Natural Science Series. (in Russian Вестник Самарского университета. Естественнонаучная серия)*, pp. 59-68.

R. von Bock und Polach, S. Ehlers, 2013. Model scale ice — Part B: Numerical model. *Cold Regions Science and Technology*, 94, pp.53–60.

Timco, G., Weeks, W., 2010. A review of the engineering properties of sea ice. *Regions Science and Technology*, 60(2), pp.107–129.

Wang J, Zhou J, Deng Y, Vadim G, Zhang P., 2020. Numerical Simulation of Ice Fractures Process of the Yellow River Based on Disk Specimen. *Crystals*, 10(7):598.